Electroclinic liquid crystals with large induced tilt angle and small layer contraction

M. S. Spector,[1] P. A. Heiney,[1,2] J. Naciri,[1] B. T. Weslowski,[1,3] D. B. Holt,[1] and R. Shashidhar[1]

[1]*Center for Bio/Molecular Science and Engineering, Naval Research Laboratory, Code 6950, Washington, DC 20375-5348*
[2]*Department of Physics and Astronomy, University of Pennsylvania, Philadelphia, Pennsylvania 19104
and Geo-Centers, Inc., 1801 Rockville Pike, Rockville, Maryland 20852*
[3]*George Mason University, Fairfax, Virginia 22030*

Optical and x-ray scattering studies of a chiral, organosiloxane smectic-*A* liquid crystal indicate a large field induced optical tilt of up to 31° accompanied by a very small contraction of the smectic layers. This result suggests that the molecules have a nonzero tilt even with no applied field, and that the primary effect of the field is to induce long range order in the direction of the molecular tilt.

I. INTRODUCTION

Chiral smectic-*A* liquid crystals which exhibit large field-induced optical tilts have been developed for potential applications in fast, gray-scale display devices [1,2]. The rotation of the optical axis arising from the coupling of a transverse dipole moment in a chiral molecule to an applied electric field is known as the electroclinic effect [3]. In most electroclinic materials, this molecular rotation is accompanied by a corresponding layer contraction which results in a buckling of the layers [4,5]. Similar layer shrinkage in ferroelectric smectic-*C** liquid crystals leads to the formation of a chevron structure [6]. The electroclinic layer buckling is easily observed in an optical microscope as periodic stripes and drastically reduces the high contrast ratio necessary for optical devices [5]. In addition, many electroclinic materials crystallize above ambient temperature making them impractical for applications [2]. Recent efforts to obtain large optical tilt angles with small layer shrinkage have focused on liquid crystals with a fluoroether tail [7] or with three ester linkages in the core and a chiral (*S*)-lactic ester in the tail [8]. Both materials exhibited very small layer contractions, with optical tilt angles up to 24° in the smectic-*C* phase of the former material and field-induced tilt angles up to 14° just above the smectic-*A* to smectic-*C** transition in the latter material.

Partial substitution of methylene groups with more flexible dimethylsiloxane groups in the alkyl chains of a ferroelectric smectic-*C** was found to suppress crystallinity and to give temperature independent tilt angles and response times [9,10]. Using this principle, Naciri *et al.* synthesized a series of organosiloxane ferroelectric liquid crystals which crystallized at low temperatures and exhibited both smectic-*A* and smectic-*C** mesophases [11]. The temperature range of the smectic-*A* phase was found to increase with the number of siloxy units, with a concurrent decrease in the smectic-*A* to smectic-*C** transition temperature [11]. These materials were found to have large electroclinic tilt angles without showing the stripe texture associated with layer buckling.

In this paper, we report on detailed electro-optic and x-ray studies on one member of this series, a liquid crystal with three dimethylsiloxane groups, focussing on the electroclinic behavior in the smectic-*A* phase. We observe field-induced optical tilt angles as large as 31° with less than a one percent contraction of the layers. Molecular modeling results indicate that the molecule is bent in the middle and the bulky siloxane tail has a hook shape. We discuss these observation in terms of simplified models for molecular rotation under an applied field.

II. EXPERIMENTAL PROCEDURE

The liquid crystal used in our studies, 4-[3′-nitro-4′-((R)-1-methylhexyloxy)phenyl]phenyl 4-(6-heptylmethyltrisiloxyhexyloxy) benzoate (TSiKN65) (Fig. 1), was synthesized and purified as previously described [11]. The phase sequence for TSiKN65 is

$$\text{smectic-}C^* \underset{25°C}{\longleftrightarrow} \text{smectic-}A \underset{56°C}{\longleftrightarrow} \text{isotropic.}$$

The melting temperature is $< -10°C$. The smectic-*C** to smectic-*A** transition temperature, T_{AC}, is somewhat higher than that previously reported due to improved sample purity [11]. The compound was loaded into a commercial liquid crystal cell (E.H.C. Co., Tokyo) with a gap of 22.5 μm. This cell had 1 cm² ITO electrodes coated with a rubbed polyimide surface layer to induce planar alignment (molecular long axis parallel to the substrate). The cell walls were chemically etched in hydrofluoric acid to a total thickness of approximately 0.3 mm to minimize x-ray absorption. The cells were mounted in an Instec MK1 hot stage and a bipolar square wave of variable amplitude was applied to the electrodes. For most measurements, the wave frequency was 100 Hz, but close to the smectic-*A*–smectic-*C** transition a 10 Hz signal was used due to the slower response of the sample.

X-ray measurements were performed in the triple-axis geometry using an Enraf-Nonius F-591 rotating anode operating at 12 kW. Germanium monochromator and analyzer crystals provided an in-plane resolution of 1.5×10^{-3} Å^{-1}
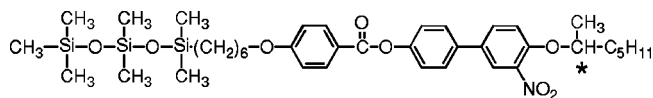
FIG. 1. The chemical structure of TSiKN65 is shown with the chiral center indicated by an asterisk.

full-width at half-maximum. Since the smectic layers were perpendicular to the cell walls, the measurements were made in transmission, with $\hat{Z}$ being parallel to the layer normal. Although a single sharp Bragg peak at the (001) position, with a mosaic of less than 1°, was always observed when cooling, we sometimes observed mosaic splittings up to 6° when heating far from T_{AC}. The sample was oriented to maximize the signal at the Bragg angle so that the peak position measured represented the true momentum transfer magnitude. Least-squares fits to a Lorentzian line shape for the (001) peak allowed us to determine the peak position to a precision of 8×10^{-5} Å^{-1}, corresponding to a fractional uncertainty $\Delta q/q = \Delta d/d = 5 \times 10^{-4}$ in peak position and layer spacing.

The rotation of the optic axis with applied field, or optical tilt, was determined by using optical transmission through crossed polarizers as previously described [12]. The light source was a stabilized halogen lamp illuminating a Nikon Optophat polarizing microscope equipped with a UDT 260 photodiode. We used the same 22.5 μm cell, with thinned glass windows, for the optical measurements that was used for x-ray diffraction measurements.

For polarizing material oriented at angle θ with respect to the first polarizer, the transmitted intensity I is given by

$$I(\theta) = I_{min} + I_0 \sin^2(2\theta)\sin^2\left(\frac{2\pi d\Delta n}{\lambda}\right) \equiv I_{min} + I_{max}\sin^2 2\theta, \tag{1}$$

where I_0 is the incident intensity, I_{min} is the background intensity observed at $\theta=0$, d is the sample thickness, Δn is the birefringence, and λ is the wavelength. If the sample is oriented at angle θ_0 with respect to the first polarizer and a square-wave electric field $E^{\pm}$ is applied, the optic axis assumes an angle $\theta^{\pm} = \theta_0 \pm \theta_{opt}$, where θ_{opt} is the optical tilt. We measure the transmitted light intensity to obtain the optical tilt:

$$I^{\pm}(\theta) = I_{min} + I_{max}\sin^2(2\theta_0 \pm 2\theta_{opt}), \tag{2}$$

where I^+ and I^- are the intensities measured when the electric field generates positive or negative optical tilts, respectively. For small optical tilts, $0 \leq \theta_{opt} \leq 11°$, maximum sensitivity is obtained by setting $\theta_0 = 22.5°$. In this case, we obtain

$$\theta_{opt} = \frac{1}{4}\left[\arcsin\left(\frac{I^+ - I_{min}}{I_{max} - I_{min}}\right) - \arcsin\left(\frac{I^- - I_{min}}{I_{max} - I_{min}}\right)\right]. \tag{3}$$

For larger tilts, $11° \leq \theta_{opt} \leq 33°$, maximum sensitivity is obtained by setting $\theta_0 = 0$, yielding

$$\theta_{opt} = \frac{1}{4}\left[\arcsin\left(\frac{I^+ - I_{min}}{I_{max} - I_{min}}\right) + \arcsin\left(\frac{I^- - I_{min}}{I_{max} - I_{min}}\right)\right]. \tag{4}$$

This technique has been extensively used in our laboratory and others to obtain precision ($\pm 0.1°$) measurements of the optical tilt [12].

Generally, it is necessary to calibrate I_{min}, I_{max}, and θ_0 only at zero field for each temperature. In the present case, we find a field dependence of I_{max} which likely arises from field-induced changes in the birefringence $\Delta n(E)$. Free rotation of the molecules about their long axis is restricted in an applied field leading to biaxiality of the system [13] and a change in the measured birefringence. This effect is known to be large in this and related materials [14,15], although we cannot completely rule out a change in the cell thickness d produced by an electromechanical expansion of the intra-plane smectic layer density and a concomitant bulging of our (thinned) cell walls. Either effect would be washed out if the light source were completely white and the photodetector response flat, but the effect of changes in $d\Delta n$ can be appreciable if these conditions are not met perfectly. Therefore, for this material it was necessary to calibrate I_{max} at each field and each temperature in order to calculate the correct optical tilt angle. We also observed that the transmitted light varied in color from green to pink with changing field.
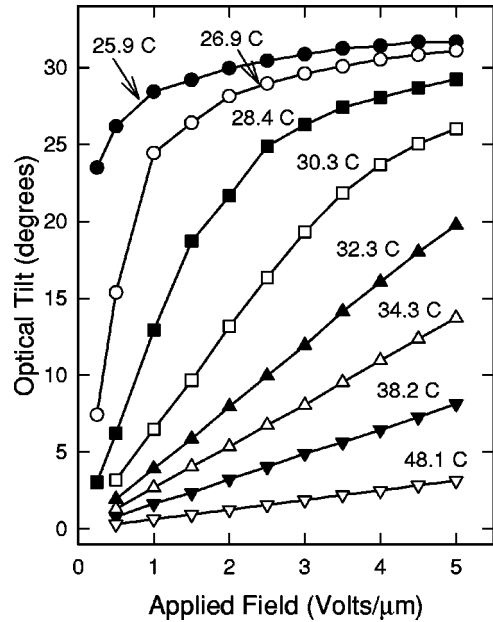
Commercial molecular modeling software was used to construct and optimize the structure of the TSiKN65 molecule [16]. Energy minimization was accomplished with semiempirical molecular orbital (MO) calculations using the AM1 Hamiltonian. An optimizer cascade consisting of steepest descents and conjugate gradient methods was employed with a rms gradient termination criterion of 0.1 kcal/(mol Å). To ensure that the best structure was obtained, dihedral energy profiles were generated for nitrobiphenyl, phenylbenzoate, phenylmethylether, and tridimethyl siloxane with AM1 MO calculations. The minimum energy bond torsions generated by the optimization of the entire TSIKN65 molecule compared favorably to the dihedrals of minimum energy in the small molecule components.

FIG. 2. Variation of optical tilt angle θ_{opt} with applied field at indicated temperatures. Solid lines are guides to the eye.

III. RESULTS

The electro-optical response of TSiKN65 at selected temperatures are shown in Fig. 2. At high temperatures in the smectic-A phase, where the optical tilt angle θ_{opt} is small, we find the expected linear increase in the θ_{opt} with applied field [3]. Closer to the A-C^* transition, the electroclinic response
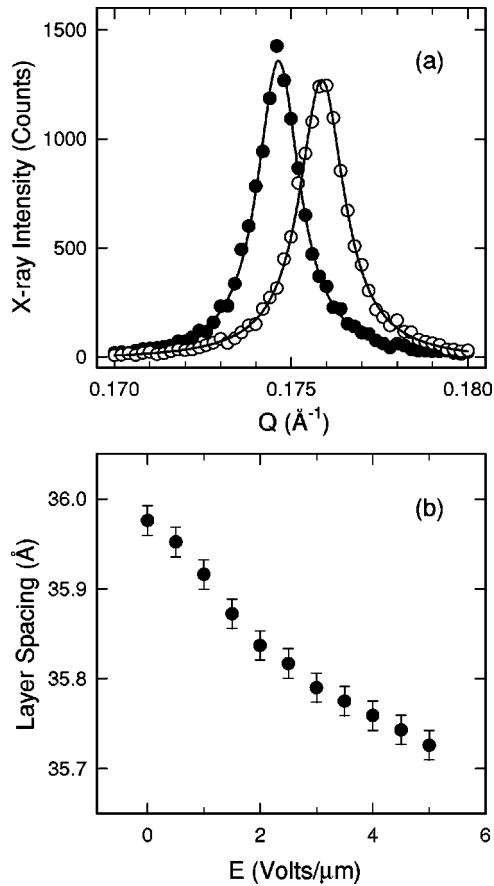
FIG. 3. (a) X-ray diffraction profiles of the (001) smectic layer peak at $T=26.9°C$ with zero applied field (solid circles) and $E=5$ V/μm (open circles). Solid lines are the results of least-squares fits to a Lorentzian profile plus a linear background. (b) Smectic layer spacing as a function of applied field at 26.9 °C, obtained from x-ray diffraction.

becomes nonlinear when $\theta_{opt}>15°$. Although θ_{opt} appears to saturate at high field close to the transition, careful examination of the data reveals that it continues to increase slowly with field. Values of θ_{opt} greater than 31° were obtained with a field of (5 V/μm) just above T_{AC}.

The results of radial ($\theta-2\theta$) X-ray diffraction measurements on TSiKN65 at 26.9 °C are shown in Fig. 3. Figure 3(a) shows the scattered intensity as a function of wave vector at 0 and (5 V/μm). The peak position shift of about one percent shown in this data is the largest field induced contraction that we measured at any temperature. The data are well fit by a Lorentzian function (lines), from which the corresponding smectic layer spacings are determined. Figure 3(b) shows the layer spacing, $d(E)$, as function of applied field. The layer spacing in the absence of field is 35.98 Å, close to the molecular length of 34.9 Å obtained from molecular modeling.

In order to compare the optical and x-ray measurements, we define the x-ray tilt as $\theta_{x\,ray}\equiv\arccos[d(E)/d_0]$, where d_0 is the smectic layer spacing in the absence of field at a given temperature. Figure 4 shows a comparison of the field dependence of θ_{opt} and $\theta_{x\,ray}$ at $T=26.9$ °C and $T=30.3$ °C. The two tilt angles have qualitatively similar behavior: they both increase with decreasing temperature, and at a given temperature exhibit an initial rapid rise followed by a gentler,
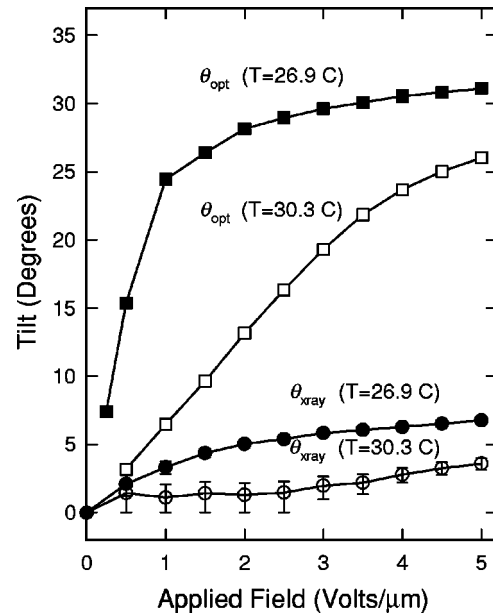
FIG. 4. Optical tilt angle θ_{opt} and x-ray tilt angle $\theta_{x\,ray}$ as a function of applied field at 26.9 and 30.3°C. Solid lines are guides to the eye.

but nonzero, continued rise with applied field. However, the x-ray tilt is always much smaller than the optical tilt, and the x-ray tilt is not simply proportional to the optical tilt.

Figure 5 shows the temperature dependence of the layer spacing at zero field and the maximum applied field of 5 V/μm. Above 35 °C there is no observable change in the layer spacing when a field is applied. Close to the transition, the layers contract up to 1% with applied field as discussed above. The zero-field layer spacing has a maximal value of 35.98 Å at $T\approx30$ °C. As T approaches $T_{AC}\approx25$ °C from above, the zero-field layer spacing decreases somewhat, most likely due to pre-transitional tilt fluctuations. As the sample is heated above 35 °C, the layer spacing again decreases, indicating a negative thermal expansion coefficient. Such behavior has previously been seen in fluorinated liquid crystals and is most likely due to increased flexibility of the hydrocarbon chain [7,17].
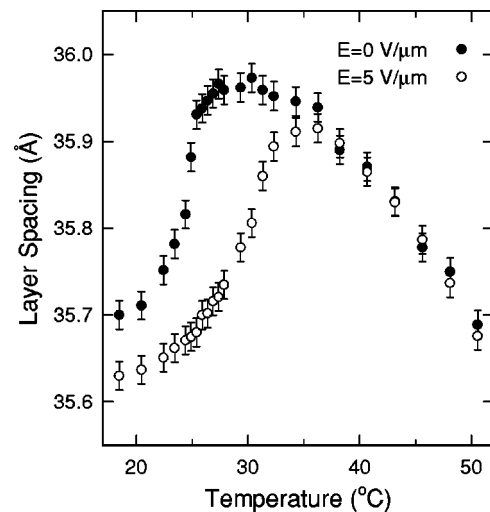
FIG. 5. Temperature dependence of the smectic layer spacing at zero field (solid circles) and at $E=5$ V/μm (open circles).
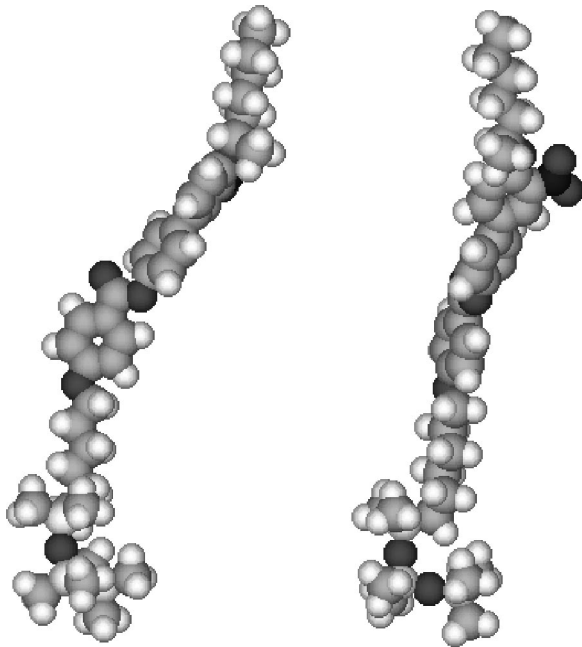
FIG. 6. Space-filling models of TSIKN65 derived from molecular modeling as described in the text. The view on the right is rotated by 60° about the vertical axis from that on the left.

Results of molecular modeling of an isolated TSIKN65 molecule are shown in Fig. 6. Several features of the minimization merit discussion. First, a bend is observed near the middle of the molecule, most clearly visible in the left view of Fig. 6. The bend angle is found to be 55° by measuring the angle between the plane containing the silicon atoms and the axis defined by the two most distant carbon atoms that are members of phenyl rings. This feature is relatively insensitive to starting parameters, and is expected to persist even in the condensed state. Second, the siloxane tail is quite bulky compared with the alkyl tail at the other end. Third, the siloxane tail is shaped like a hook, as seen most clearly in the right-hand view of Fig. 6. The minimum-energy structure of the siloxane tail of TSIKN65 is similar to that of tridihydrosiloxane obtained with *ab initio MO* calculations [18]. In this model molecule, the hook shape is generated by a *trans-cis* sequence of Si-O-Si-O and O-Si-O-Si dihedrals. For the tridimethylsiloxane tail, the general hook shape is retained, but the dihedral sequence is closer to a *gauche-cis* conformation which relieves steric repulsions between methyl groups. We note, however, that angle bending and torsional potential surfaces for siloxanes are generally shallow over wide deformations [18,19]. This confers a high degree of flexibility to siloxane materials, and the conformation of the siloxane material in the condensed state may very well be different from the minimum-energy state of an isolated molecule.

Depending on its conformation, the siloxane tail may have a sizable static dipole moment, comparable to those of the atoms in the nitro group. For example, in our energy minimization, the siloxane tail had a static dipole moment of 0.35 D, to be compared with 6.2 D for the nitrobiphenyl group and 7.7 D for the molecule as a whole. Combined with the flexibility of the siloxane tail, electric field-induced conformational changes in the tail are possible.

IV. DISCUSSION

We now discuss the microscopic interpretation of our results. The observations we wish to reconcile are the following: (1) In the smectic-A phase close to T_{AC}, the optical tilt rises rapidly with applied field from 0 to around 28° and then continues to increase more slowly, achieving a value of 31.1° at 5 V/μm. (2) The x-ray layer spacing has qualitatively similar behavior, with an initial rapid rise followed by a slow increase. However, the maximum x-ray tilt is approximately 6.7°. A similarly large optical tilt accompanied by a small decrease in layer spacing were recently observed by Radcliffe *et al.* in the smectic-C phase [7]. As originally proposed by de Vries [20], they suggested that the molecules are tilted at all temperatures, and that the optical tilt arises from the development of long range order in azimuthal orientation. In this section we discuss the advantages and disadvantages of a variety of simplified models for the molecular order.

(i) Rigid rod model: In the most naive approach to the A-C^* transition, the molecules are treated completely as rigid rods characterized by polar angle η and azimuthal angle ϕ, and the A-C^* transition consists of a rotation of the rod director from $\eta=0$ to a finite value, with a spontaneously broken symmetry in ϕ. The same rotation can be achieved in the smectic-A phase by the application of an electric field, which also breaks the symmetry in ϕ [Fig. 7(a)]. In this model, the optic axis is colinear with that of the entire molecule so that $\theta_{opt}=\theta_{x\,ray}=\eta$. Such a relationship is very nearly followed in some materials, including a closely related electroclinic liquid crystal [12,21], but a rigid rod model is clearly ruled out for TSiKN65 by the large discrepancy in our measured values of θ_{opt} and $\theta_{x\,ray}$.

(ii) Rigid rod plus interdigitation: One way to overcome the contradiction in model (I) would be to postulate that the layers are initially interdigitated, but separate as the layer tilt increases so that the change in the total layer spacing is small [Fig. 7(b)]. However, this model, although not invalidated by the data, seems implausible. Optical and x-ray tilts of 31° and 6.7°, respectively, correspond to 14 and 0.7% decreases in layer spacing. For this model to be correct, we would have to assume that the layers fortuitously deinterdigitate by exactly the right amount to cancel out the effect of molecular tilt to better than 1%.

(iii) Molecular hinge: Another explanation for the discrepancy between optical and x-ray tilt angles could arise from the flexibility of the molecule. We assume a segmented molecule [Fig. 7(c)], in which only the optically active portion B (of length L_1), is allowed to tilt, while portions A and C (of total length L_2) are always parallel to the layer normal. In this model, $\theta_{opt}=\eta$ and $\theta_{x\,ray}$ is determined by the net layer contraction. We can calculate the value of L_1 by inserting maximal optical and x-ray tilt angles of 31° and 6.7° and the length of the untilted molecule:

$$L_1+L_2=L=35.98 \text{ Å}, \tag{5}$$

$$L_1 \cos \theta_{opt}+L_2=L \cos \theta_{x\,ray} \tag{6}$$

to obtain $L_2=1.7$ Å. This is far too short to be a reasonable estimate of the optically active portion of the molecule.

(iv) Azimuthal order: As originally suggested by de Vries [20], a very small decrease in layer spacing upon cooling
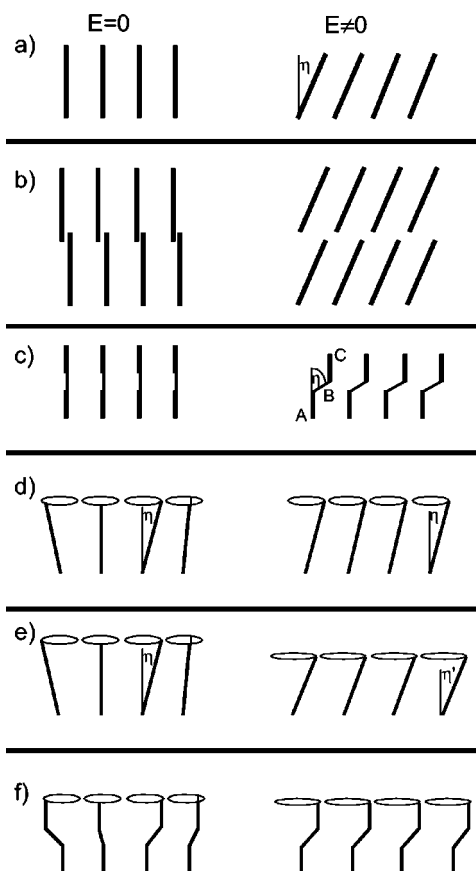
FIG. 7. Schematic models for the molecular ordering. The left column shows the hypothesized structure with zero electric field, and the right column that with a large applied field perpendicular to the plane of the paper. (a) Rigid rod tilting with the optic axis coincident with the molecular axis. (b) The same as (a), but with a decrease in interdigitation compensating for the decrease in layer thickness. (c) Molecular hinge model, in which only the optically active part of the molecule tilts upon application of a magnetic field. (d) Rotator model, in which rods are always tilted by the same angle η and the optical tilt is a consequence of development of long-range azimuthal order. (e) The same as (d), except that the field also induces a small change in tilt, $\eta' > \eta$. (f) The same as (e), except the shape of the molecule is more correctly represented as having a sickle shape, which gives rise to a larger tilt of the upper, optically active portion relative to the lower, bulky portion containing the siloxane groups.

into the smectic-C phase or, in our case, upon application of an electric field, could arise if the molecules are always tilted on a cone of angle η, and the transition consists of the development of long-range order in ϕ [Fig. 7(d)]. de Vries proposed a sliding phase in which the tilt directions were uncoupled in adjacent layers of the smectic-A phase. Such a sliding phase has recently been theoretically investigated [22] and observed in simulations [23,24]. Alternatively, one could just as easily have short-range tilt order within each layer. If η were completely field invariant, of course, then $\theta_{\text{x ray}}$ would always be zero, but it is easy to incorporate a weak coupling between η and ϕ such that the layers contract by roughly 1% during the development of azimuthal orientational order [Fig. 7(e)].

(v) This interpretation can be improved with a more microscopic model of the molecule. As discussed above, molecular modeling indicates that the siloxane groups are both bulky and flexible, and that there is a pronounced bend near the center of the molecule so that the entire molecule is shaped more or less similar to a sickle. One can anticipate that the bulky siloxane groups will pack tightly, and be resistant to field-induced tilt, while the tilted portion of the molecule, including the optically active section, will have enough room to rotate easily [Fig. 7(f)]. Furthermore, under an applied electric field, the appreciable dipole moment of the siloxane tail will result in a torque tending to counteract that of the nitro group, so that the entire molecule is more likely to rotate about its long axis (ϕ) rather than to tilt about a short axis (η). More detailed molecular calculations in the condensed state would be necessary to establish the actual extent of steric hindrance, but simulations of a simplified system of ''bent rods'' [24] show that steric repulsion alone can be enough to drive a A-C transition.

More realistically, of course, multiple effects are probably present. The molecules are flexible, and their conformation must surely change upon application of an electric field. Furthermore, there is surely some interdigitation, although the predicted sign of the interdigitation change upon applied field is not immediately obvious. However, a modified version of model (iv) or (v) still provides the best overall explanation for our data.

In conclusion, we have observed large field induced optical tilt in a chiral, organosiloxane smectic-A liquid crystal. The large tilt is accompanied by a very small layer contraction. We interpret these results as arising primarily from the development of azimuthal orientational order in molecules which are already tilted in the absence of electric field. This property should allow for the development of electroclinic devices free from defects due to layer buckling typically observed in materials with large layer contraction.

[1] P.A. Williams, N.A. Clark, M. Blanca Ros, D.M. Walba, and M.D. Wand, Ferroelectrics **121**, 143 (1991).

[2] B.R. Ratna, G.P. Crawford, S.K. Prasad, J. Naciri, P. Keller, and R. Shashidhar, Ferroelectrics **148**, 425 (1993).

[3] S. Garoff and R.B. Meyer, Phys. Rev. Lett. **38**, 848 (1977); Phys. Rev. A **19**, 338 (1979).

[4] J. Pavel and M. Glogarová, Ferroelectrics **114**, 131 (1991); Liq. Cryst. **9**, 87 (1991).

[5] K. Skarp, G. Andersson, T. Hirai, A. Yoshizawaa, H. Takezoe, and A. Fukuda, Jpn. J. Appl. Phys. **31**, 1409 (1992).

[6] T.P. Rieker, N.A. Clark, G.S. Smith, D.S. Parmar, E.B. Sirota, and C.R. Safinya, Phys. Rev. Lett. **59**, 2658 (1987); N.A. Clark

and T.P. Rieker, Phys. Rev. A **37**, 1053 (1988).

[7] M.D. Radcliffe, M.L. Brostrom, K.A. Epstein, A.G. Rappaport, B.N. Thomas, R. Shao, and N.A. Clark, Liq. Cryst. **26**, 789 (1999).

[8] F. Giesselmann, P. Zugenmaier, I. Dierking, S.T. Lagerwall, B. Stebler, M. Kašpar, V. Hamplová, and M. Glogarová, Phys. Rev. E **60**, 598 (1999).

[9] K. Sunohara, K. Takatoh, and M. Sakamoto, Liq. Cryst. **13**, 283 (1993).

[10] H.J. Coles, H. Owen, J. Newton, and P. Hodge, Liq. Cryst. **15**, 739 (1993).

[11] J. Naciri, J. Ruth, G. Crawford, R. Shashidhar, and B.R. Ratna, Chem. Mater. **7**, 1397 (1995).

[12] G.P. Crawford, R.E. Geer, J. Naciri, R. Shashidhar, and B.R. Ratna, Appl. Phys. Lett. **65**, 2937 (1994).

[13] F. Yang and J.R. Sambles, Liq. Cryst. **13**, 1 (1993).

[14] J.R. Lindle, F.J. Bartoli, S.R. Flom, J.V. Selinger, R. Shashidhar, and B.R. Ratna, Mater. Res. Soc. Symp. Proc. **559**, 33

(1999).

[15] R. Bartoli and J.R. Lindle (private communication).

[16] Molecular modeling employed *HyperChem*, version 5.1, HyperCube, Inc.

[17] P. Mach, P.M. Johnson, E.D. Wedell, F. Lintgen, and C.C. Huang, Europhys. Lett. **40**, 399 (1997).

[18] S. Grigoras and T.H. Lane, J. Comput. Chem. **9**, 25 (1988).

[19] S. Grigoras and T.H. Lane, J. Comput. Chem. **8**, 84 (1987).

[20] A. de Vries, Mol. Cryst. Liq. Cryst. **41**, 27 (1977).

[21] R.E. Geer, S.J. Singer, J.V. Selinger, B.R. Ratna, and R. Shashidhar, Phys. Rev. E **57**, 3059 (1998).

[22] C.S. O'Hern, T.C. Lubensky, and J. Toner, Phys. Rev. Lett. **83**, 2745 (1999).

[23] F. Affouard, M. Kroger, and S. Hess, Phys. Rev. E **54**, 5178 (1996).

[24] J. Xu, R.L.B. Selinger, J.V. Selinger, B.R. Ratna, and R. Shashidhar, Phys. Rev. E. **60**, 5584 (1999).